



Efficient adsorption of RhB using Moroccan natural clay: equilibrium, kinetic, thermodynamic, and theoretical study

Othmane Lamrani¹ · Karim Tanji² · Haounati Redouane³ · Youssef Fahoul² · Mohammed Belkasmi⁴ · Abdellah Boushaba¹

Received: 28 November 2022 / Accepted: 29 April 2023 / Published online: 1 June 2023
© Springer Nature Switzerland AG 2023

Abstract

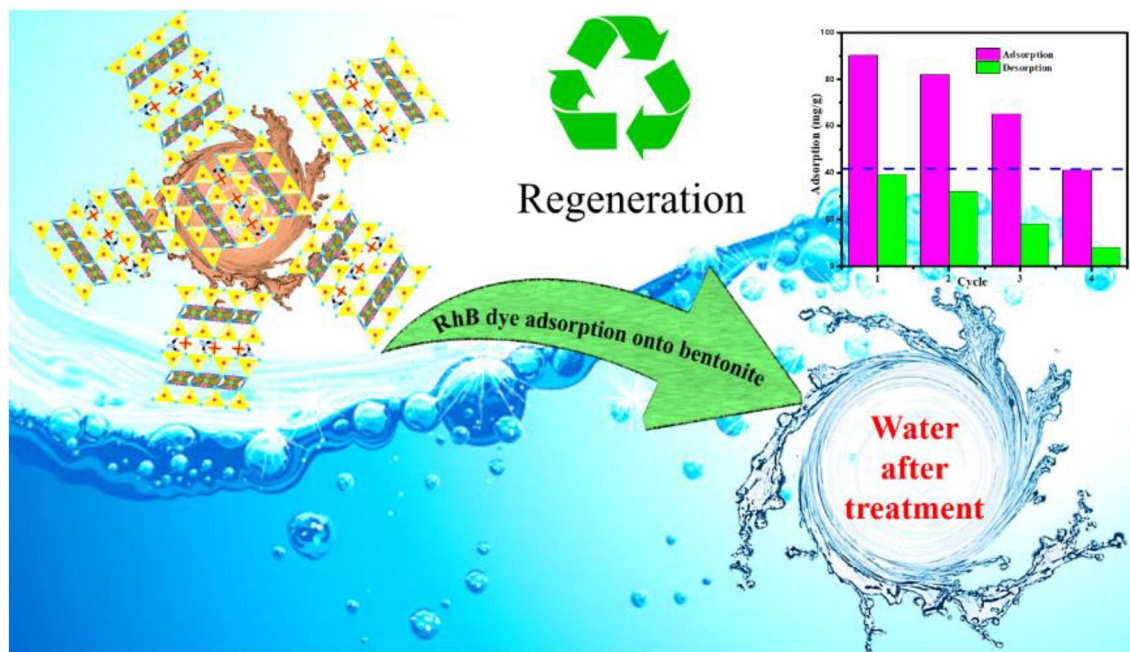
This study aims mainly to examine the potentiality of using raw natural adsorbent (bentonite) as an inexpensive solid adsorbent for the adsorption of rhodamine B (RhB), which is essentially a cationic dye, in a batch system. The physicochemical properties of bentonite have been determined by X-ray fluorescence, X-ray diffraction, scanning electron microscopy, and Fourier transform infrared spectroscopy. The natural bentonite contains montmorillonite, illite, quartz, and calcite as major phases. The influence of operating conditions such as the solution pH, the dye concentration, the adsorbent mass, the particle diameter, and the temperature of the reaction medium was investigated. The maximum adsorption efficiency of up to 97% for 50 min was obtained at a low initial RhB concentration of 30 mg/L, pH 10, a temperature of 328 K, and a granulate diameter of 63 μm . The kinetic rate of the RhB adsorbed onto the bentonite was well modeled by a pseudo-second-order model. Additionally, the results illustrate that the Langmuir model perfectly describes the adsorption process with $R^2=0.99$. The thermodynamic (ΔG° , ΔH° , and ΔS°) parameters indicate that the adsorption processes were spontaneous, endothermic, and random in the adsorption process. The adsorption of the RhB dye on the bentonite surface could be carried out by electrostatic attractions and hydrogen bonds. On the other hand, Monte Carlo coupled with the simulated annealing algorithm (SAA) is used. The simulation was carried out to more clearly, on an atomic scale, reveal the interfacial interactions between RhB molecule and adsorbent surface. It was found that the simulation data correlate well with actual results.

Communicated by Mohamed Ksibi.

✉ Karim Tanji
karim.tanji@usmba.ac.ma

- ¹ Laboratory of Natural Substances, Faculty of Sciences Dhar El Mahraz, Pharmacology, Environment, Modeling, Health & Quality of Life (SNAMOPEQ), University Sidi Mohamed Ben Abdellah, Fez, Morocco
- ² Laboratory of Catalysis, Process, Materials and Environment, Higher School of Technology of Fez, University Sidi Mohamed Ben Abdellah, Fez, Morocco
- ³ Physical Chemistry and Environment Team, Faculty of Science, Ibn Zohr University, Agadir, Morocco
- ⁴ Laboratoire de Géosciences, Environnement, Faculty of Sciences Dhar El Mahraz, Ressources Associées, Sidi Mohamed Ben Abdellah University, Fez, Morocco

Graphical Abstract



Keywords Adsorption · Rhodamine B · Bentonite · Langmuir · Desorption · Monte Carlo

Introduction

Nowadays, a large quantity of wastewater contains dyes that come largely from the textile industry (Mbognou et al. 2022). Therefore, textile dyeing processes as well as the chemical content of dyeing components are very important (Haounati et al. 2021a). The dye wastewater contains acids, bases, dissolved solid toxic compounds, and considerable color pollutants. Moreover, many dyes are toxic, obstruct catalytic effects, and also cause severe damage to human bodies, preventing light penetration, reducing photosynthetic activity, and inhibiting biota growth (Baskaralingam et al. 2006; Alakhras et al. 2020; Tanji et al. 2023a). Rhodamine B (RhB) has the properties of mild washing and light fastness on wool. This is also an effective analytical reagent for metal identification (Ahmad et al. 2015; Vakili et al. 2014; Heibati et al. 2014; Oyekanmi et al. 2019). Nevertheless, the use of RhB as a food color has been banned for many years because of its alleged carcinogenic and hormonal disturbance effects in addition to being neurotoxic and genotoxic (Combes and Haveland-Smith 1982; Azeez et al. 2020; Rabti et al. 2019). Wastewater that comes from the textile, leather, paper, and printing industries contains toxic dyes that have been discharged into the environment without or

with insufficient treatment (Haounati et al. 2022; Kassimi et al. 2021).

Many researchers have examined dye removal from aqueous solution using catalytic wet peroxide oxidation, photocatalytic degradation (Belghiti et al. 2022; Gaidoumi et al. 2021; Dra et al. 2020a; Fahoul et al. 2022; Haounati et al. 2021b; Tanji et al. 2023b, 2023c), coagulation/flocculation (Verma et al. 2012), etc. Although the adsorption process has been employed extensively with various natural materials, according to the literature, few studies have been performed to investigate the removal of RhB by using raw bentonite as a natural adsorbent. The most widely used adsorbents are the following: zeolites, goethite, clays (Hadri et al. 2022; Dra et al. 2020b; Thiam et al. 2020), and bacterial biomass (Jiang et al. 2020; Ouachtak 2020; Cheng et al. 2020). Bentonite is increasingly used as an adsorbent in wastewater treatment due to its wide availability, low cost, and good intrinsic adsorption characteristics. It is one of the most commonly used adsorbents due to its net negative surface charge, making it an efficient adsorbent for the removal of cationic dyes and other organic pollutants (Toor et al. 2015; Mrabet et al. 2021a).

Morocco is a North African country, bound to the north by the Mediterranean Sea and to the west by the Atlantic Ocean. This transitional location between the African, European, and American plates provides it with richness,

diversity, and geomorphological complexity (Fullea et al. 2010). Over time it has undergone several orogenic cycles, each involved, through its geodynamic context and its scope, in the shaping the three major structural areas, which permit us to classify Morocco as an excellent natural geology laboratory. The formation of mineralized bodies is sometimes intimately mixed with that of host rocks and is often accompanied by meteoric or hydrothermal alteration of these rocks with the sharing of elements. On the other hand, mineralized bodies such as bentonites appear as an intruder in the middle of their geological surroundings. As an important clay mineral, bentonites consist of mainly montmorillonite, which is also the main component of weathered crust elution-deposited rare earth ores; they have been widely used in industrial applications (Haounati et al. 2021b) because of their specific characteristics including large surface area, high selectivity, chemical stability, adsorption properties, low cost, and high abundance (Ouachtak et al. 2020). In addition, clays can retain inorganic and organic pollutants and stop the circulation of contaminated fluids in both aquatic and soil environments (Kausar et al. 2019; Mrabet et al. 2021b).

To the best of our knowledge, and according to an extensive literature review, no previous studies have been carried out on the combination of experimental and theoretical data on the adsorption of RhB dye on Moroccan bentonite clay. The novelty of this study is based on the use of abundant and inexpensive (bentonite) for the removal of hazardous RhB dye and the theoretical explanation of the mechanism of adsorption by molecular dynamics simulation, to study the dynamic behavior of bentonite/RhB water systems to better understand the adsorption mechanism. It is well known that the removal of organic-based pollutants is generally related to their adsorption onto the used support surface, which underlines the key role of adsorbate/adsorbent interactions in this process (Achour et al. 2018; Souza et al. 2018). Recently, computational modeling has been served to investigate, at atomic and electronic scales, several adsorbate/adsorbent depollution systems (Haouti et al. 2019). Among applied modeling tools, Monte Carlo simulation was coupled with the simulated annealing algorithm (MCS-SAA) (Abdellaoui et al. 2021a, 2021b). This modeling approach is employed to evaluate explicitly the interfacial adsorbate/adsorbent interactions at an atomic scale via the adsorption energy and the adsorption geometry (Laabd et al. 2021).

The present paper aims to investigate the adsorption capacity of a natural adsorbent, and its characterization as an eco-friendly element to remove hazardous RhB from aqueous solutions. The effect of operational parameters on RhB adsorption such as the amount of natural adsorbent, initial dye concentration, particle size, temperature, pH, and toxicity tests was investigated. Alongside the experimental study, the adsorption mechanism of RhB on the employed

clay substrate was computationally explored by Monte Carlo simulation coupled with the simulated annealing algorithm.

Materials and methods

Materials

The studied natural bentonite as adsorbent for RhB removal was taken from North Region of Morocco (Fig. 1). This type of clay mineral originated from different types of weathering of Neogene volcanic and volcano-sedimentary formations (Ddani et al. 2005). From a mineralogical point of view, the bentonites are basically composed of kaolinite/smectite, illite, and montmorillonite, wherein the crystallochemical composition ranges from montmorillonite to beidellite (Lamrani et al. 2021). Indeed, the bentonite ore deposits of the eastern Rif Belt are commonly distributed around several volcanic eruptions, such as the Gourougou stratovolcano and its satellite massifs (e.g., Tidiennit rhyolitic massif), with significant economic potential (Lamrani et al. 2021).

The dye examined in this study is rhodamine B (RhB). The characteristics of the dye are summarized in Table 1.

Characterization techniques

X-ray fluorescence (XRF) was used to explore the chemical composition of raw bentonite. The X-ray diffractometer (X'PERT PRO) was equipped with a detector operating at 40 kV and 30 mA with CuK α radiation ($\lambda = 1.540598 \text{ \AA}$), and the FTIR spectra were recorded with a VERTEX 70 at a resolution of 4 cm^{-1} with 20 scans in the $4000\text{--}400 \text{ cm}^{-1}$ wavenumber range. Scanning electron microscopy (QUANTA 200) was used to identify the composition and the morphological surface of the natural adsorbent.

The average crystallite sizes (D) were calculated using the Scherrer equation:

$$D = K\lambda / (\text{FWHM} \times \cos \theta) \quad (1)$$

where $K = 0.9$ is the shape factor, λ is the X-ray radiation wavelength, FWHM is the full width at half maximum of all characteristic peaks, and θ is the diffraction angle.

pH_{PZC} determination

The pH_{PZC}, the pH at which the bentonite surface has zero net charges, was determined by stirring 0.15 g of natural adsorbent and 50 mL of 0.01 M NaCl solution for 48 h. The initial pH values were adjusted (in the pH range from 2 to 12) using HCl or NaOH solutions. The final pH was measured after 48 h under agitation at room temperature. The point of zero charges of the natural adsorbent (pH_{PZC}) is the

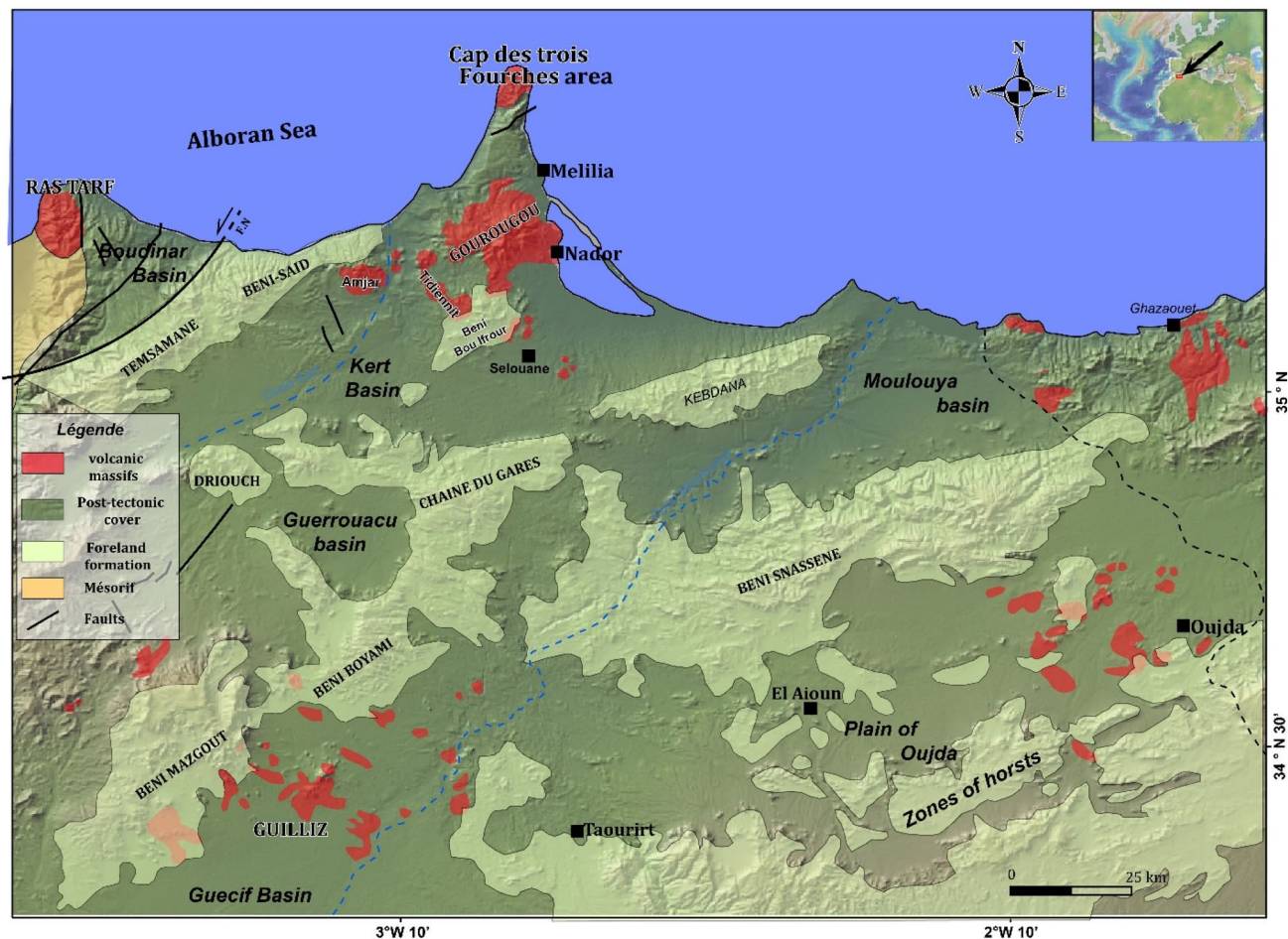


Fig. 1 Geological map of northeastern Rif Belt (Bakkali et al. 1998)

Table 1 Properties and molecular structures of rhodamine B

Properties	RhB
Chemical formula	$C_{28}H_{31}ClN_2O_3$
Wavelength	554 nm

point where the curve pH_{final} versus $pH_{initial}$ crosses the line $pH_{initial} = pH_{final}$ (Mragui et al. 2017).

Adsorption study

The adsorption batch experience was executed by introducing a mass of the adsorbent in the solution of RhB under magnetic stirring. A sample was collected each 5 min to measure its residual concentration using a UV–visible spectrophotometer (VR-2000) at a wavelength of 554 nm. Nevertheless, before the measure, the suspension was centrifuged to separate the natural adsorbent from the RhB liquid. The RhB removal was calculated using Eq. (2) (Senthil Kumar et al. 2010), where, C_0 and C_t are the concentration of RhB

at $t=0$ and $t \neq 0$, respectively. The adsorption capacity of the sediment for RhB removal was obtained by applying Eq. (3), Where q_e (mg/g) is the adsorption capacity at the equilibrium; C_0 (mg/L) is the initial concentration of RhB; C_e (mg/L) is the equilibrium concentration of RhB; V (L) is the RhB solution volume; m (g) is the natural adsorbent mass (Lian et al. 2009).

$$\text{Removal (\%)} = \frac{(C_0 - C_t)}{C_0} \times 100 \quad (2)$$

$$q_e = \frac{(C_0 - C_t)}{C_0} \times V \quad (3)$$

Computational details

To clarify the interfacial interactions between the RhB molecule and the employed clay substrate (i.e., bentonite), the MCS-SAA is used (Kirkpatrick et al. 1979). The heating

process consisted of three heating cycles with 15,000 steps per cycle. As the clay essentially contained montmorillonite (Mt), a cell of $25.9 \text{ \AA} \times 44.9 \text{ \AA} \times 96.6 \text{ \AA}$ including 60.0 \AA as a sufficient vacuum region above the substrate composed of three Mt(001) layers was used. The appropriate (hkl) Miller index for the Mt substrate was determined using the Bravais–Friedel–Donnay–Harker algorithm (Bourzi et al. 2020). The molecular modeling process was conducted under the periodic boundary conditions and setting atom- and Ewald-based summation as methods to estimate Van der Waals and electrostatic interactions, respectively. The geometry optimization was carried out using the smart algorithm with 0.001 kcal/mol , 0.5 kcal/mol/\AA , and 0.015 \AA as convergence criteria for energy, force, and displacement, respectively. Prior to starting adsorption, the geometry of RhB was optimized using the COMPASS force field. Excepting the above indications, the rest of the parameters' values were default ones in Materials Studio 6.0 software. The adsorption energy (E_{ads}) of the target pollutant inhibitor on Mt(001) surface is calculated using the following formulae:

$$E_{\text{Ads}} = E_{\text{Total}} - (E_{\text{Mt}(001)} + E_{\text{Ads}}^{\text{RhB}}) \quad (4)$$

where, $E_{\text{Mt}(001)}$, $E_{\text{Ads}}^{\text{RhB}}$, and E_{Total} energetic components denote the energy of Mt(001) substrate with preadsorbed species, adsorbed RhB molecule, and energy of the whole system, respectively.

Results and discussions

Adsorbent characterization

The mineralogical characterization of the raw bentonite as a natural adsorbent was investigated using X-ray diffraction as a rapid analytical technique. As can be seen in Fig. 2,

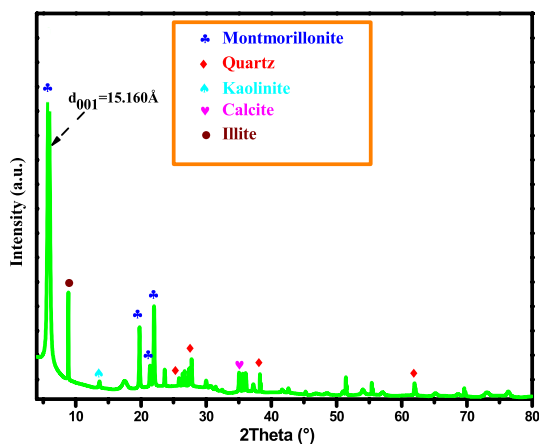


Fig. 2 X-ray diffraction of the raw natural bentonite

and according to JCPDS file N° 012–0232, the bentonite is essentially composed of montmorillonite with the characteristic peak located at $2\theta = 5.742^\circ$ corresponding to the basal spacing of 15.160 \AA . However, the other peaks are impurities corresponding to illite at $2\theta = 8^\circ$, calcite (CaCO_3) at 2θ equal to 35.15° , and quartz (SiO_2) at 2θ equal to 25.50° and 37.43° . The low peak located at 2θ equal to 14.27° reveals the presence of kaolinite fraction (Qihaa et al. 2016; Miz et al. 2017). The calculated average crystallite size of the bentonite is $11 \mu\text{m}$.

The scanning electron microscopy (SEM) analysis (QUANTA 200), made on the natural adsorbent before adsorption (Fig. 3a and b), shows that the natural adsorbent has a homogeneous surface, which could favor the RhB molecules' fixation on the natural adsorbent surface. Hence, the selected SEM images after the RhB adsorption display an irregular adsorbent surface that could be explained by the saturation of the adsorbent active sites (Fig. 3c and d).

The purpose of the FTIR analysis is to confirm the structure of the adsorbent before and after adsorption. Figure 4 shows the characteristic bands of the natural raw adsorbent. These bands are attributed to the Si–O, Si–O–M, M–O–H (M = Al, Fe, and Mg) bonds existing between the anions and cations located in octahedral or tetrahedral sites, as well as a large number of OH groups. The absorption bands observed clearly confirm the presence of the bonds characterizing bentonite. The band located in the interval $3200\text{--}3600 \text{ cm}^{-1}$ corresponded to OH frequencies of the water molecule (Alabarse et al. 2011). The spectrum of bentonite shows two absorption bands, one in the range of $800\text{--}1200 \text{ cm}^{-1}$ and the other centered on 500 cm^{-1} characteristics of the stretching vibrations of the Si–O bond. Usually, in bentonite, this band appears at 1100 cm^{-1} . This slight shift toward low frequencies is due to the presence of trivalent ions (Al^{3+}) in the tetrahedral sites substituted for silicon and ferric ions in octahedral sites. Moreover, the displacement of the peaks exceeds the field of 900 cm^{-1} , thus characterizing the iron at 3600 cm^{-1} , which proves the presence of Mg in the structure of the analyzed bentonite adsorbent (Reddy et al. 2009; Qabaqous et al. 2014). After the adsorption of hazardous RhB dye into bentonite, as can be seen in the FTIR spectrum two bands appeared at 1586 cm^{-1} and 1365 cm^{-1} , which are attributed to the C=C stretching vibration of the RhB benzene ring and to the C–C aromatic stretching of RhB dye, respectively. Thus, it can be concluded that the adsorption of hazardous RhB dye is due to the interactions between RhB molecules and the adsorbent active sites.

Analysis of the X-ray fluorescence results obtained for the fractions of the raw bentonite with a diameter of less than $63 \mu\text{m}$ shows that the predominant oxide is SiO_2 (58.92%), Al_2O_3 (25.21%), Fe_2O_3 (3.63%), and other impurity oxides (Na_2O , K_2O , MgO , and CaO) present in a small percentage (Table 2).

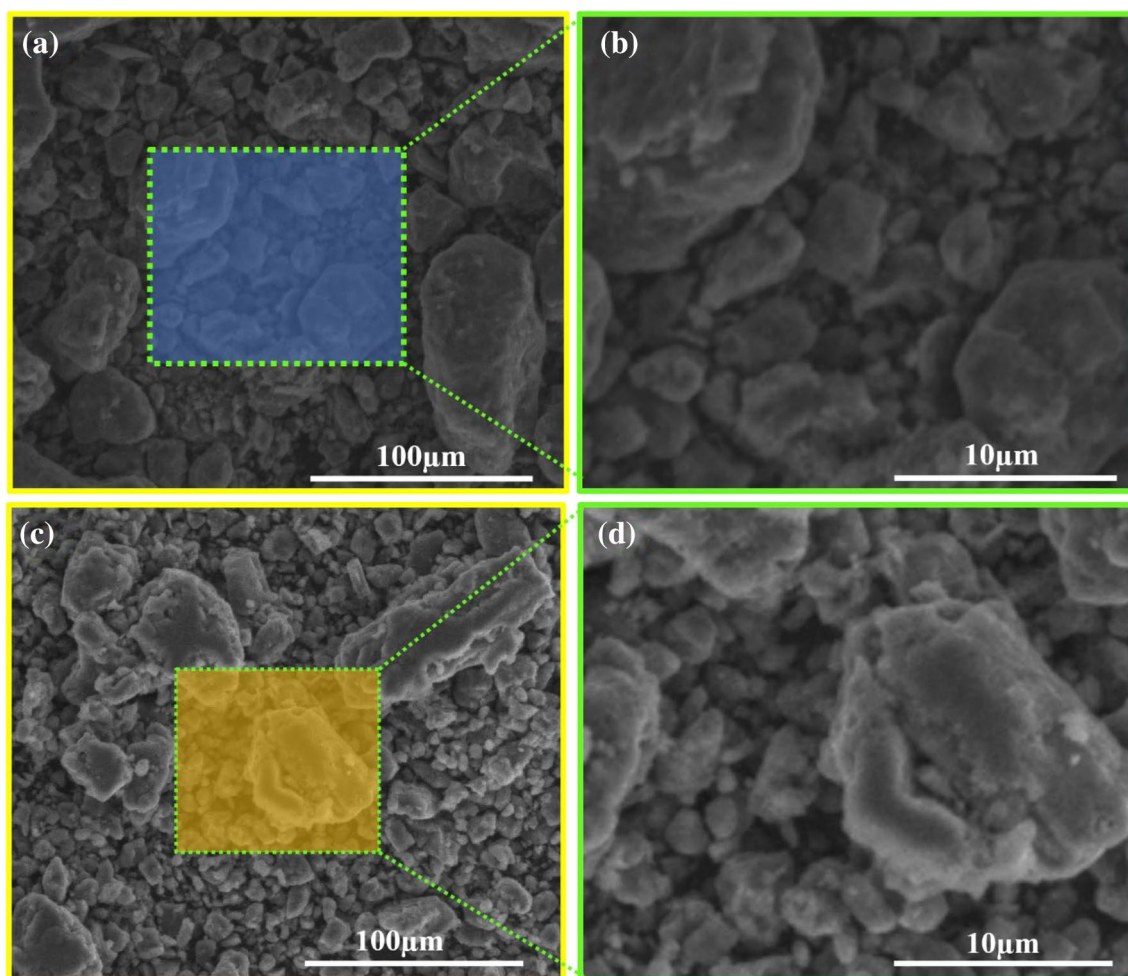


Fig. 3 SEM images of raw natural adsorbent: **a** $\times 1000$ and **b** $\times 4000$ before adsorption; **c** $\times 1000$ and **d** $\times 4000$ after adsorption

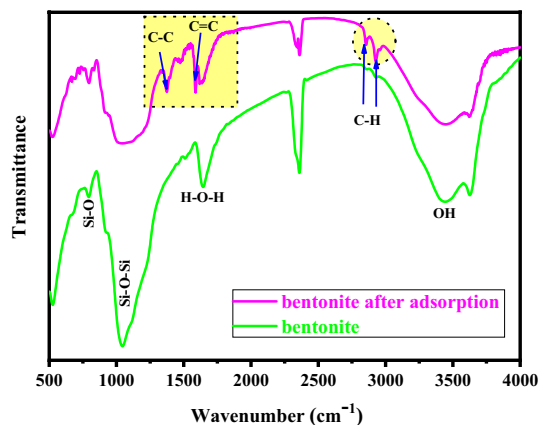


Fig. 4 FTIR spectrum of raw bentonite adsorbent

Effect of different parameters on the adsorption efficiency

This study evaluates the influence of adsorbent mass to determine its role in the adsorption process. Figure 5 illustrates the RhB removal variation as a function of the adsorbent's dose, which varies from 0.5 to 3 g/L, using 40 mg/L as the RhB concentration at room temperature displays an enhancement in RhB removal with the increase of the natural adsorbent mass from 53% to 92% when the mass of the adsorbent increases from 0.5 to 3 g. This result could be explained by the increase in the mass of the adsorbent, as more adsorbent active sites are provided for RhB adsorption, resulting in improved adsorption of RhB molecules into the active sites of the adsorbent (Dhahir et al. 2013).

Furthermore, Fig. 5b illustrates the intersection point of the adsorption capacity and the removal efficiency of RhB at different adsorbent mass values (0.5–3 g) that correspond to 1 g/L. This mass was taken as an optimal adsorbent mass used in the other tests.

The initial RhB concentration is one of the most significant parameters influencing the adsorption efficiency. To study this factor, the initial RhB concentration effect was monitored at varying initial RhB concentrations between 10 and 60 mg/L, using 1 g of natural adsorbent at room temperature for 50 min. According to Fig. 6a, in the area of lower concentrations, there is a rapid increase in the RhB removal. The removal decreases with the increase in the RhB initial concentration, which could be explained by the presence of solid interactions between the adsorbent surface and the RhB molecules; afterward the RhB removal becomes stable

due to the saturation of the active sites on the adsorbent surface, which eventually leads to a decrease in the removal efficiency (Dali Youcef et al. 2019). Figure 6b shows the intersection point of adsorption capacity and the removal curves as a function of the equilibrium concentrations. It can be seen that, when the initial concentration increases, the adsorbed amount increases while the efficiency of elimination decreases.

To investigate the adsorbent particle size influence on the RhB adsorption efficiency, a series of experiments were carried out with different particle diameters (40, 63, 125,

Table 2 Chemical composition of raw bentonite clay

Constituent	SiO ₂	Al ₂ O ₃	Fe ₂ O ₂	CaO	MgO	Na ₂ O	K ₂ O	TiO ₂	MnO	P ₂ O ₅	LOI
Constituent (%)	58.92	25.21	3.63	1.31	2.37	1.89	0.82	0.20	0.01	0.04	5.60

LOI loss on ignition

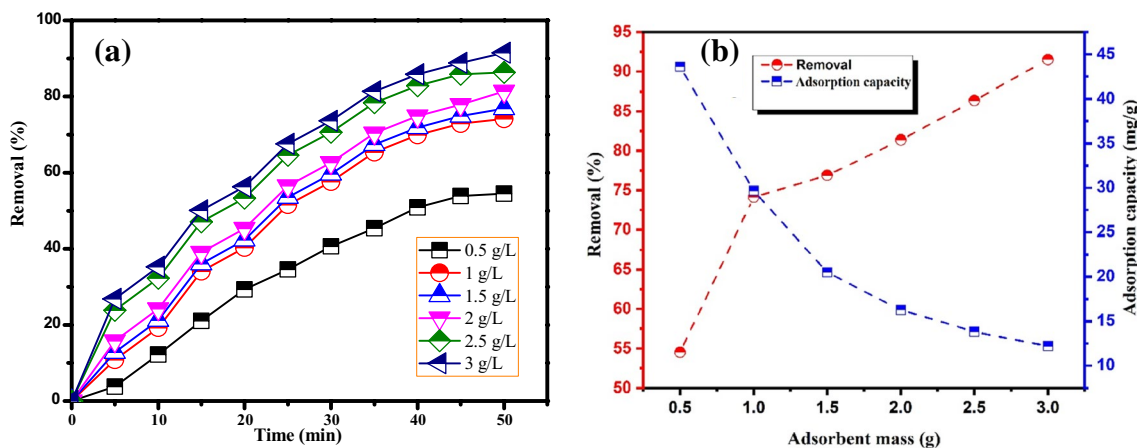


Fig. 5 a Raw bentonite adsorbent mass effect on the RhB adsorption; b The intersection points of adsorption capacity and the removal efficiency during the adsorption phenomenon at different adsorbent mass values

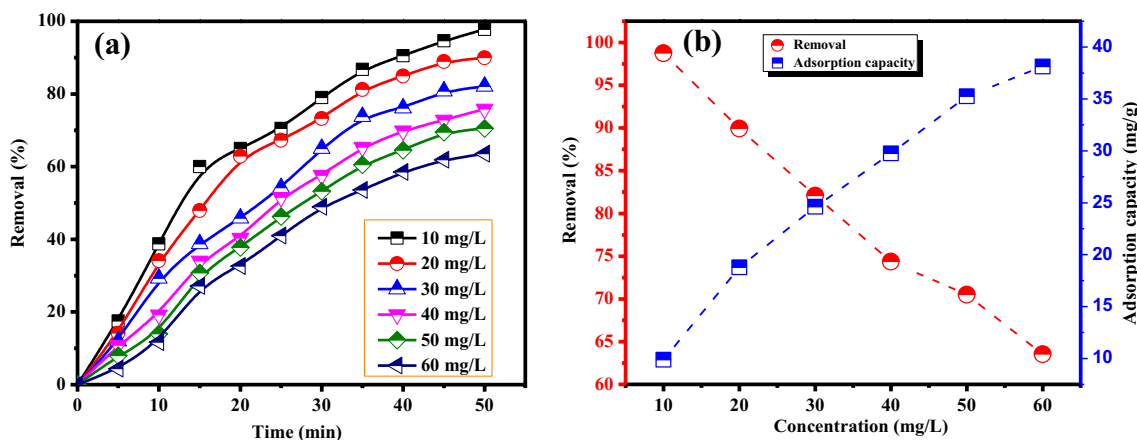


Fig. 6 a Initial RhB concentration effect on the adsorption process; b the intersection points of adsorption capacity and the removal efficiency during the adsorption phenomenon

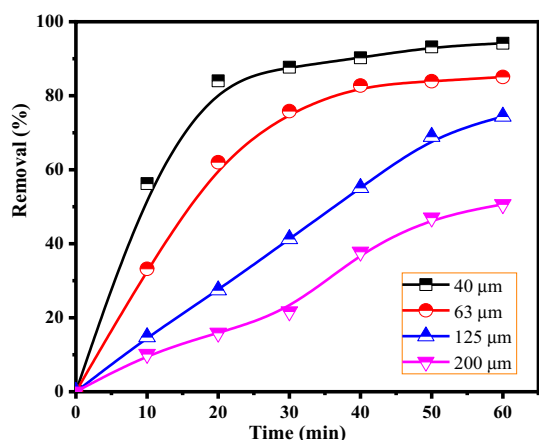


Fig. 7 RhB removal at different particle sizes of bentonite adsorbent

and 200 μm) using 1 g of natural adsorbent and 30 mg/L as RhB initial concentration at room temperature. Figure 7 illustrates that decreasing particle size enhanced the removal of RhB dye: the highest RhB removal (92%) was obtained with 40 μm , while the lowest removal (64%) was remarked with 200 μm . This result is due to the effect of reducing the size of particles increasing the adsorbent surface area and thus providing more active sites for RhB adsorption, which ultimately ameliorates the adsorption efficiency (Chen et al. 2018).

Figure 8 shows the influence of temperature on hazardous RhB dye adsorption onto bentonite adsorbent, where removal efficiency is enhanced from 74% to 81% by increasing the temperature from 298 to 328 K. This result confirms that the adsorption process is endothermic and requires high energy to achieve the equilibrium at low temperatures. This evolution could be justified by the augmentation of the adsorbent active sites or by the decrease in the thickness of the adsorbent, and consequently the decrease in the mass

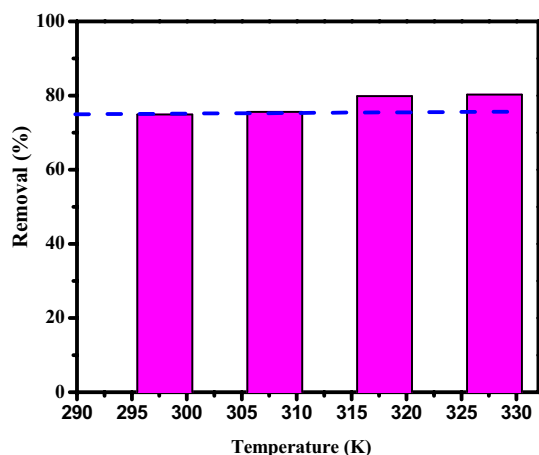


Fig. 8 Effect of temperature on RhB adsorption

transfer resistance of the adsorbate in the boundary layer (Hu et al. 2006).

The effect of solution pH on the adsorption efficiency was investigated by varying pH values from 4 to 10, using optimal conditions. The obtained result displayed in Fig. 9 indicates that the RhB removal increases from 50% to 90% by increasing the pH from 4 to 10. The natural adsorbent surface charge depends on the solution pH: in basic pH, the surfaces are negatively charged because of the abundance of OH^- ions, which cause an electrostatic attraction between the negatively charged natural adsorbent surface and the cationic RhB dye to ameliorate the adsorption of RhB onto the adsorbent. As a result, maximum removal of RhB by natural adsorbent occurred at basic pH of 10 (Hu et al. 2006; Gupta et al. 2004; Singh et al. 2003).

The effect of solution pH could be explained by the change in the surface charge of bentonite as a function of pH. At a pH higher than pH_{PZC} ($\text{pH} > \text{pH}_{\text{PZC}}$) the surface charge of bentonite is negative, which promotes attraction between the RhB and the adsorbent. At pH lower than pH_{PZC} ($\text{pH} < \text{pH}_{\text{PZC}}$) the surface charge of bentonite is positive (same charge as the dye RhB), which explains the small adsorbed quantity of RhB by the effect of electrostatic repulsions (Haouti et al. 2019; Akhouairi et al. 2019). Figure 10 shows that the point of zero-charge pH_{PZC} of the raw bentonite adsorbent is 8.01. The effect of solution pH could explain that the natural adsorbent surface was negative at its pH greater than pH_{PZC} , which favored the attraction between the RhB and the adsorbent.

Kinetic models

The pseudo-first-order model is presented by Lagergren's relation in the form of Eq. (5), if the Lagergren relation is verified, by carrying $\ln(q_e - q_t)$ as a function of time. The pseudo-second-order (PSO) kinetic model was also investigated using

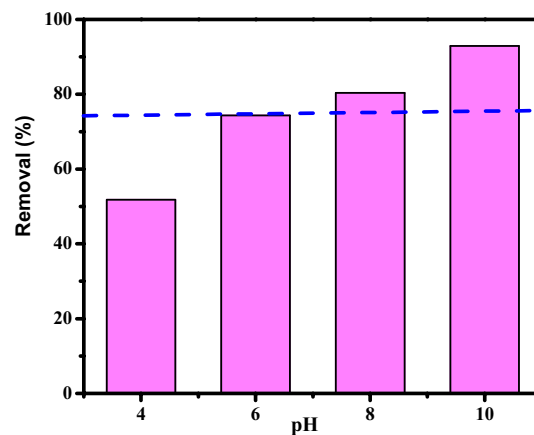


Fig. 9 Effect of initial solution pH on the adsorption process

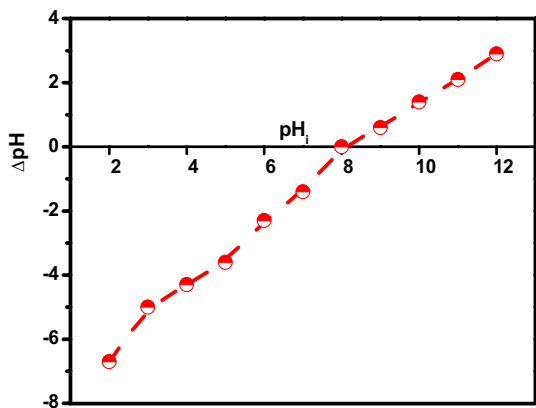


Fig. 10 The graphical presentation of pH_{PZC} of raw bentonite

Eq. (6), in which q_e is the adsorption capacity at equilibrium, q_t is the adsorption capacity at different times, k is the kinetic constant, and t is the time (Leodopoulos et al. 2012).

$$\ln (q_e - q_t) = \ln (q_e) - k_1 t \tag{5}$$

$$\frac{t}{q_t} = \frac{1}{k_2 q_e^2} + \frac{t}{q_e} \tag{6}$$

It can be seen in Fig. 11a, b and Table 3 that the values of the pseudo-first-order (PFO) R^2 were 0.67, 0.59, 0.79, 0.71, and 0.81; and the values of the pseudo-second-order (PSO) R^2 were 0.997, 0.998, 0.981, 0.992, and 0.991. According to these results, the adsorption process is in good agreement with (PSO) kinetic, which was the main kinetic process as long as it gives the best prediction for the kinetic data. Therefore, the rate-limiting step may be chemisorption, which involves valence forces by sharing or electron exchange between the adsorbent and the adsorbate (Taylor et al. 2014).

Isotherm adsorption

Concerning the adsorption isotherm study, the Langmuir and Freundlich models were examined and applied to describe the adsorption process. The Langmuir isotherm is one of the models that describe monolayer adsorption. It assumes a homogeneous adsorption surface with binding sites having equal energy. The linear form of the Langmuir isotherm

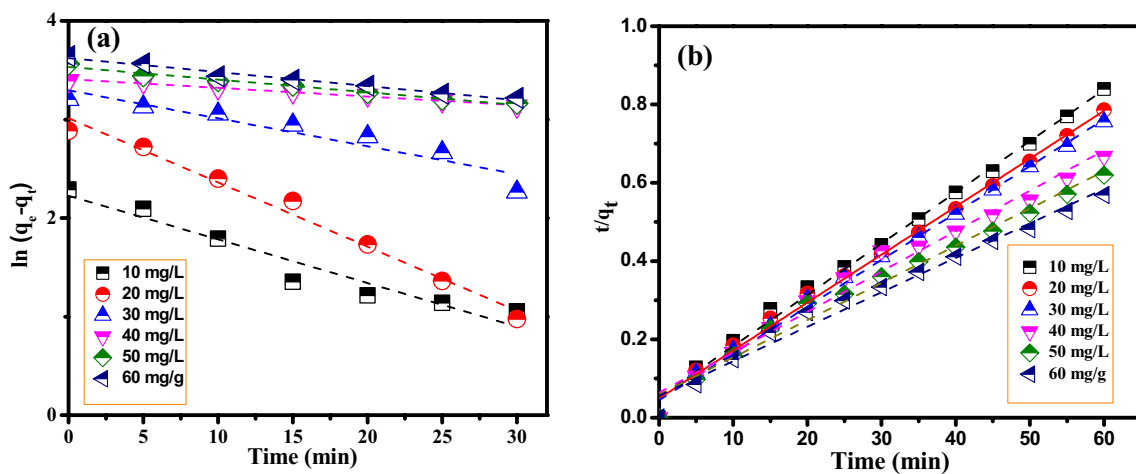


Fig. 11 Kinetic models for adsorption RhB dye onto bentonite. a Pseudo-first order mode; b pseudo-second order model

Table 3 Pseudo first-order and pseudo second-order parameters for adsorption of Rhodamine B molecules onto bentonite at different concentrations

RhB Concentration (mg/L)	q_e , experimental (mg/g)	Pseudo-first order			Pseudo-second order		
		k_1 (min^{-1})	q_e , calculated (mg/g)	R^2	k_2 (g/mg.min)	q_e calculated (mg/g)	R^2
10	9.87	$8.7 \cdot 10^{-3}$	3.78	0.67	$9.10 \cdot 10^{-4}$	8.84	0.99
20	18.67	$7.2 \cdot 10^{-3}$	9.25	0.59	$8.9 \cdot 10^{-4}$	18.07	0.99
30	24.73	$1.9 \cdot 10^{-2}$	15.13	0.79	$6.2 \cdot 10^{-4}$	22.39	0.98
40	32.11	$4.9 \cdot 10^{-2}$	19.39	0.71	$5.1 \cdot 10^{-4}$	31.38	0.99
50	35.7	$6.4 \cdot 10^{-2}$	24.01	0.81	$3.1 \cdot 10^{-4}$	34.45	0.99
60	38.97	$9.4 \cdot 10^{-2}$	26.67	0.75	$1.6 \cdot 10^{-4}$	37.67	0.98

can be expressed as Eq. (7), where C_e is the equilibrium concentration (mg/L), q_e and q_m are the equilibrium and maximum adsorption capacity (mg/g), respectively, and K_L is the Langmuir constant (L/mg) (Foo and Hameed 2010; Ayawei et al. 2017).

The Freundlich model describes non-uniform and multilayer adsorption on heterogeneous surfaces; Eq. (8) is its corresponding equation, where, K_f is the adsorption capacity, and $1/n$ is the intensity of adsorption (Foo and Hameed 2010; Ayawei et al. 2017; Mohamed and Ouki 2011); these constants are associated with the Freundlich isotherm model. The exponent ($1/n$) gives an indication about the capacity and the favorability of the adsorbent/adsorbate system; the increasingly large K_f value indicates greater adsorption capacity (Azeez et al. 2018, 2022a, 2022b). The corresponding data of the two models are presented in Table 4 and Fig. 12. Concerning adsorption isotherm study, the Langmuir and Freundlich models

$$\frac{C_e}{q_e} = \frac{C_e}{q_m} + \frac{1}{K_L \cdot q_m} \quad (7)$$

$$\log q_e = \log K_f + \frac{1}{n} \log C_e \quad (8)$$

Based on the higher value of R^2 and the lowest χ^2 , which is considered an indicator of the good fitness of experimental data with the isotherm models, the obtained results from

isotherm adsorption indicate that the adsorption process of RhB onto the bentonite correlated more with Langmuir isotherm ($\chi^2 = 71.026$, $R^2 = 0.998$) (Eq. (7)) than Freundlich (Eq. (8)) isotherm. This result indicates that the RhB dye can be adsorbed homogeneously by active receptor sites on the surface of the bentonite adsorbent and a saturated adsorption capacity is expected due to limited adsorptive sites on the surface.

Adsorption thermodynamic studies

The effect of temperature on the removal efficiency was carried out in the temperature range of $T = 298\text{--}328$ K. However, the type of sorption could be investigated through such thermodynamic quantities as Gibbs free energy (ΔG° , kJ/mol), the enthalpy change (ΔH° , kJ/mol), and entropy change (ΔS° , kJ/mol/K), and the experimental data were obtained using the following equations:

$$\Delta G^\circ = -RT \ln K_e \quad (9)$$

$$\ln K_e = \frac{\Delta S^\circ}{R} - \frac{\Delta H^\circ}{RT} \quad (10)$$

$$\Delta G^\circ = \Delta H^\circ - T\Delta S^\circ \quad (11)$$

where K_e° is the adsorption equilibrium constant that is obtained from the Langmuir model, R is the universal gas constant (8.314 J/mol/K), and T is the absolute temperature

Table 4 Adsorption isotherm constants for RhB adsorption onto the raw natural adsorbent (related to Fig. 12)

Langmuir isotherm parameters				Freundlich isotherm parameters			
q_m (mg/g)	K_L	R^2	χ^2	$1/n$	K_f	R^2	χ^2
29.33	1.268	0.998	71.026	0.953	1.482	0.756	97.631

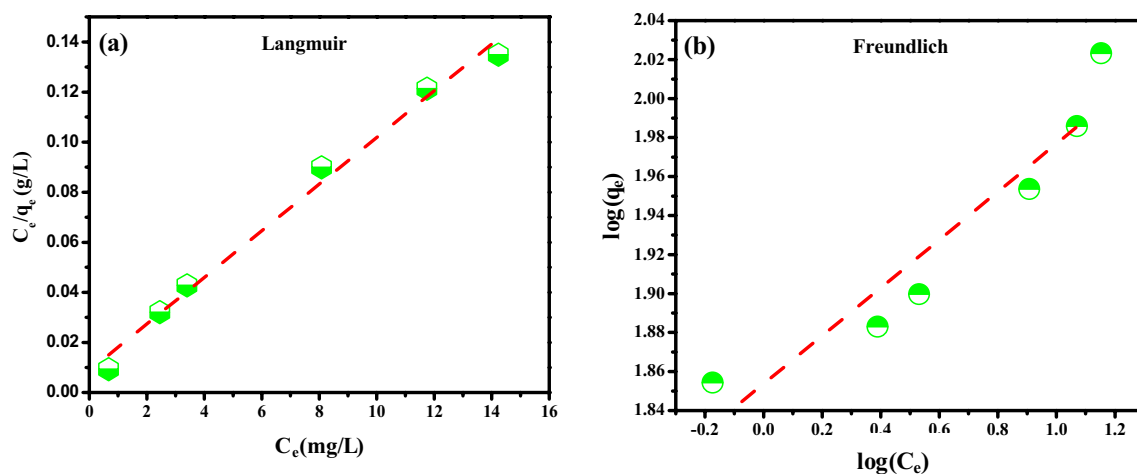


Fig. 12 Isotherm model for adsorption of RhB onto bentonite. **a** Langmuir; **b** Freundlich

(K). As can be observed in Fig. 13a, the adsorption capacity of RhB dye has significantly increased from 5 to 15.5 mg/g as the temperature increased in the range of 298–338 K. Therefore, this behavior indicates that the RhB adsorption reaction occurring on the bentonite's surface is endothermic, which explains that at each temperature increase, the removal of hazardous RhB dye becomes more and more favorable. As it is shown in both Fig. 13b and Table 5, the obtained negative values of free energy ΔG° at 298, 308, 318, and 328 K indicate the spontaneous nature of the adsorption (Bulut and Aydin 2006). The positive ΔH value of 5.78 kJ/mol confirmed the endothermic adsorption nature of RhB, while the slightest ΔS value of 0.018 kJ/mol/K reveals an increase of the randomness at the RhB–natural adsorbent solution interface during the adsorption process (Namasivayam and Kavitha 2002).

Proposed adsorption mechanism

The mechanism of rhodamine B adsorption into bentonite can be investigated by electrostatic interactions (Fig. 14). As previously mentioned, bentonite clay was shown to contain many kinds of functional groups such as silanol Si–OH and aluminol Al–OH. However, the electrostatic interactions between the positively charged RhB dye ($-N^+-(CH_3)_2$) and the negatively charged groups (Si–O⁻ and Al–O⁻) present at the edges of bentonite surface sites. The hydrogen bond between the H⁺ atoms of the layer (Si–OH and Al–OH) and the nitrogen atoms of rhodamine B can also explain the mechanism adsorption phenomena of the RhB dye by bentonite clay. Therefore, the excellent adsorption capacity of bentonite for RhB is due to the presence of both functional groups silanol Si–OH and aluminol Al–OH.

Table 5 Thermodynamic parameters of RhB adsorption onto the bentonite

ΔH (kJ/mol)	ΔS (kJ/mol/K)	ΔG (kJ/mol) 298 (K)	ΔG (kJ/mol) 308 (K)	ΔG (kJ/mol) 318 (K)	ΔG (kJ/mol) 328 (K)
21.68	0.12	-14.08	-15.28	-16.48	-17.6

Reutilization studies

The frequent reusability of adsorbents to remove organic pollutants in wastewater is a key factor for judging its efficiency and reducing wastewater treatment cost. In the present work, the reuse tests were performed during four successive adsorption/desorption cycles for the removal of RhB with an initial concentration of 30 mg/L from an aqueous solution onto 1 g/L bentonite using 50% ethanol–water (v/v), at 25 °C during 2 h. However, before its reuse, it is necessary that the adsorbent be washed several times with water. The desorption percentage was calculated on the basis of the analysis of dye concentration recovered after the washing step.

As can be seen in Fig. 15, the adsorption efficiency after four cycles runs was decreased from 91% to 42%. This behavior was attributed to the fact that the adsorbate molecules (RhB) that are positively charged were strongly attached to the bentonite surface, which is negatively charged possibly via chemical adsorption.

Computational results

To investigate the adsorption process of RhB dye on the Bt-based adsorbent, leading to its removal from the solution, molecular modeling at the atomic scale was performed employing Monte Carlo simulation coupled with SAA. In

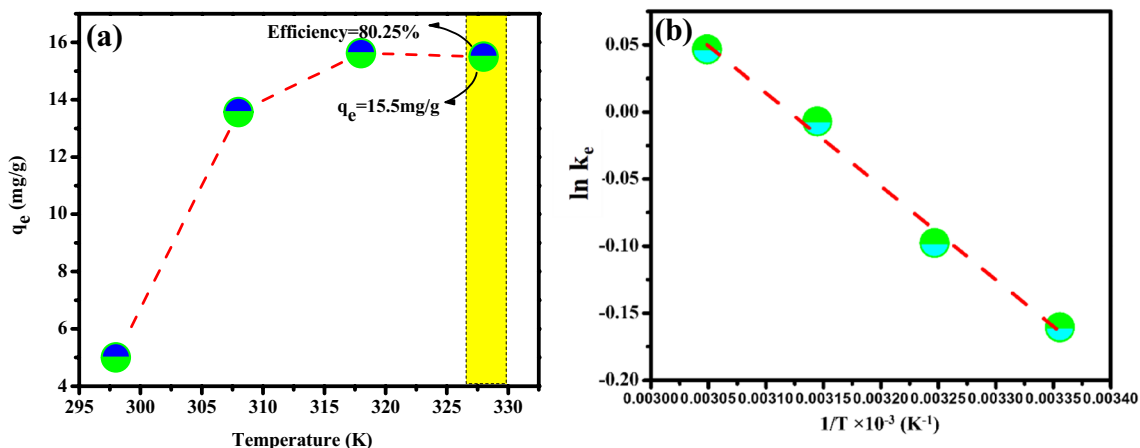


Fig. 13 **a** The effect of temperature on the adsorption of RhB dye onto bentonite; **b** Van't Hoff plot of removal of RhB dye onto bentonite

Fig. 14 Proposed mechanisms for the adsorption of rhodamine B dye on bentonite

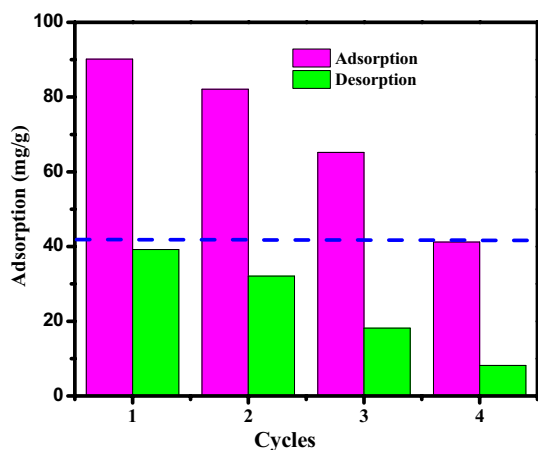
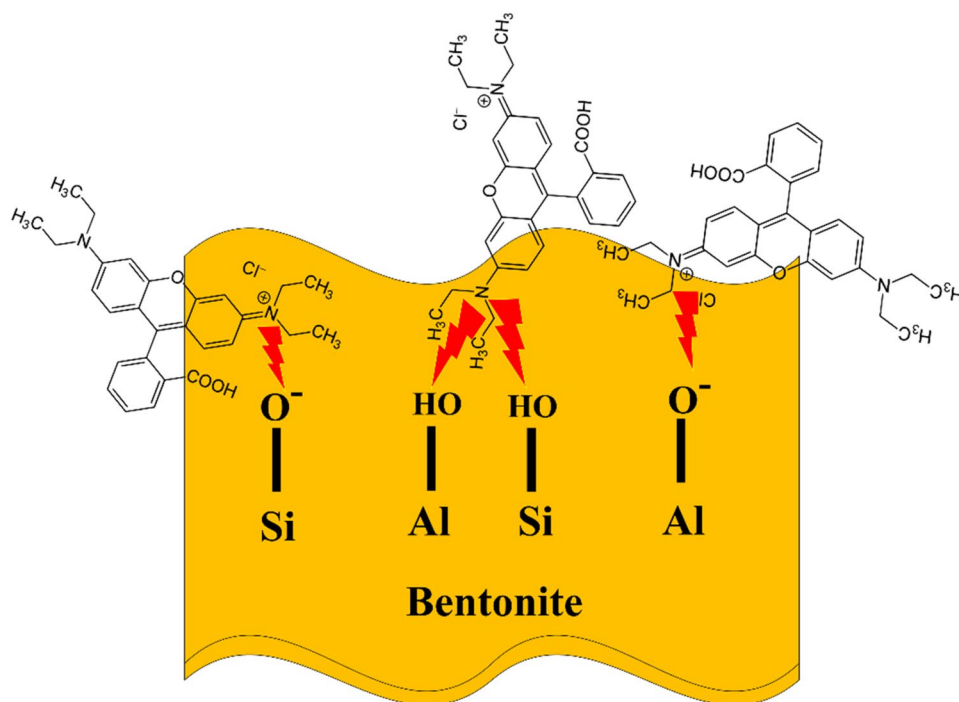


Fig. 15 RhB adsorption during the regeneration cycles of the bentonite

this regard, the interfacial RhB@Bt interaction is discussed in terms of its energetic and geometric aspects in the current subsection. Based on the most stable RhB@Bt adsorption geometry, the calculated adsorption energy is -764.179 kcal/mol. The magnitude and sign of this energy value confirm the stability of the acquired adsorption system and also indicate the affinity of the RhB molecule to adsorb onto Bt(001) surface. This can be explained by the implication of strong electrostatic interactions in this process between the RhB molecule and the substrate surface, which reinforce the adsorption of the target pollutant on the bentonite surface (Abdellaoui et al. 2021a, 2021b). Figure 16 shows the most

stable adsorption geometry of the RhB molecule onto the bentonite surface, as well as its field density. As a result, the RhB molecule is found to be placed on the substrate surface through a flat adsorption orientation (i.e., parallel adsorption), which indicates its affinity to adsorb onto the used adsorbent. Furthermore, it can be seen that almost all heteroatoms (O and N) spread on the RhB molecule are directed toward the substrate surface, which signifies their effective implication on the interfacial RhB@Bt(001) interactions, leading to strong adsorption (Laabd et al. 2021). Meanwhile, the inspected adsorption configuration runs in parallel with the discussed energetic aspect of the adsorption process of RhB on the Bt surface. Overall, the present computational findings confirm the acquired experimental data from which higher RhB removals are attained using bentonite adsorbent.

Comparison of the treatment efficiency and cost analysis with literature studies

Table 6 presents the adsorption efficiency of RhB using different clays reported by some literature studies (Khan et al. 2012; Hou et al. 2011; Huang et al. 2017; Khudhair and Al-Rudaini 2017; Singh et al. 2018) compared with the results obtained in the present work. The results obtained by other works showed that the dye removal varies between 19% and 94.2% within a contact time range of 40–80 min. Hence, Moroccan natural adsorbent could be a promising natural adsorbent for the elimination of RhB in aqueous solutions with RhB removal of 97% during 50 min.

The cost analysis of the application of natural bentonite was assessed and compared with previous works using natural and prepared adsorbents for the removal of RhB (Table 7). As natural bentonite is freely available, the purchase cost is 0 US\$; however, the cost of transportation was found to be 5 US\$/kg. Hence, the cost of bentonite was highly competitive compared with other adsorbents' costs (Inyinbor et al. 2016; Bello et al. 2019, 2020; Adegoke et al. 2022). Moreover, it is about 55 times

cheaper than commercial activated carbon, which costs only 273 US\$/kg.

Conclusion

The present paper reveals that the natural adsorbent bentonite, unlike other adsorbents, has potential to be used for removing RhB. The experimental results have shown that

Fig. 16 **a** Top and **b** side views of the most stable adsorption configuration of RhB onto Bt(001) surface. **c** Density of the adsorbate component (grid resolution 0.4 Å)

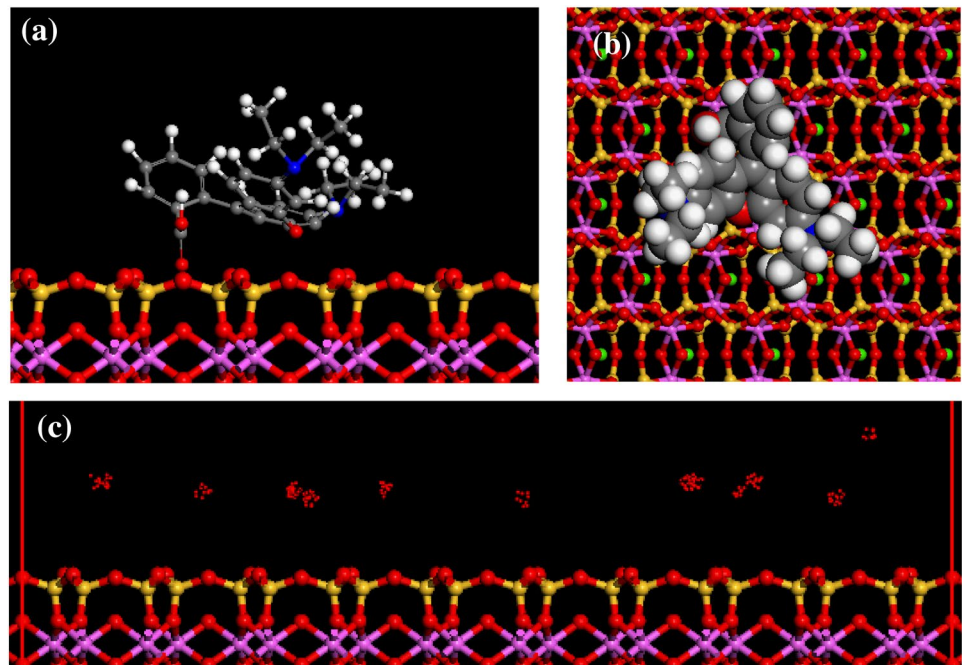


Table 6 Comparison of the treatment efficiency of RhB on different adsorbents with some literature studies

Adsorbent	Adsorbent dose (g/L)	RhB concentration (mg/L)	Adsorption capacity (mg/g)	Removal (%)	Contact time (min)	Reference
Moroccan bentonite	1	30	29.33	97	50	Present work
Kaolinite	3	90	46.08	83	80	Khan et al. 2012
Gaozhou natural adsorbent	1.5	10	N.A	19	40	Hou et al. 2011
CTAB-natural adsorbent	1	350	173.5	94.2	40	Huang et al. 2017
Rhamnus stone	0.35	20	9	83	70	Khudhair and Al-Rudaini 2017
Banana peel powder	13.33	25	3.8	81.07	60	Singh et al. 2018

Table 7 Comparison costs of adsorbents used for RhB removal

Adsorbent	Cost (US\$/kg)	Reference
Epicarp of <i>Raphia hookerie</i> fruits	0.021	Inyinbor et al. 2016
Activated carbon prepared from locust bean husk	42.52	Bello et al. 2019
Activated carbon derived from <i>Gmelina aborea</i> leaves	36.34	Bello et al. 2020
Acid-modified mango pod (AMMP)	34.30	Adegoke et al. 2022
Natural bentonite	5	The present study

the maximum removal is obtained at an initial RhB concentration of 30 mg/L, pH of 10, equilibrium contact time of 50 min, temperature of 298 K, and natural adsorbent dose of 1 g/L. Experimental data were adequately interpreted by Langmuir isotherm and pseudo-second-order kinetics. The thermodynamic study has shown that the adsorption process is endothermic and spontaneous for the tested temperatures. It would be interesting to continue testing other compounds having an attractive potential on the surface of the natural adsorbent and the RhB in an aqueous solution. The affinity of the target dye to adsorb onto the used adsorbent was confirmed using Monte Carlo simulation, revealing an high adsorption energy of -764.179 kcal/mol. Finally, this study proved the efficiency of a natural adsorbent RhB dye, which encourages its use as a cost-effective and eco-friendly adsorbent for the removal of RhB dye from wastewater.

Funding This research received no specific grant from any funding agency in the public, commercial, or not-for-profit sectors.

Data availability Not applicable.

Declarations

Conflict of interest The authors declare that they have no known competing financial interests or personal relationships that could have appeared to influence this paper.

References

- Abdellaoui Y, Abou Oualid H, Hsini A, El Ibrahim B, Laabd M, El Ouardi M, Giacomán-Vallejos G, Gamero-Melo P (2021a) Synthesis of zirconium-modified Merlinoite from fly ash for enhanced removal of phosphate in aqueous medium: experimental studies supported by Monte Carlo/SA simulations. *Chem Eng J* 404:126600. <https://doi.org/10.1016/j.cej.2020.126600>
- Abdellaoui Y, El Ibrahim B, Abou Oualid H, Kassab Z, Quintal-Franco C, Giacomán-Vallejos G, Gamero-Melo P (2021b) Iron-zirconium microwave-assisted modification of small-pore zeolite W and its alginate composites for enhanced aqueous removal of As(V) ions: experimental and theoretical studies. *Chem Eng J*. <https://doi.org/10.1016/j.cej.2021.129909>
- Achour Y, Khouili M, Abderrafia H, Melliani S, Laamari MR, El Haddad M (2018) DFT investigations and experimental studies for competitive and adsorptive removal of two cationic dyes onto an eco-friendly material from aqueous media. *Int J Environ Res* 12(6):789–802. <https://doi.org/10.1007/S41742-018-0131-X>
- Adegoke KA, Adeleke O, Adesina MO, Adegoke RO, Bello OS (2022) Clean technology for sequestering Rhodamine B dye on modified mango pod using artificial intelligence techniques. *Curr Res Green Sustain Chem* 5:100275. <https://doi.org/10.1016/j.crgsc.2022.100275>
- Ahmad A, Mohd-Setapar SH, Chuong CS, Khatoon A, Wani WA, Kumar R, Rafatullah M (2015) Recent advances in new generation dye removal technologies: novel search for approaches to reprocess wastewater. *RSC Adv* 5:30801–30818. <https://doi.org/10.1039/c4ra16959j>
- S. Akhouairi, H. Ouachtak, A.A. Addi, A. Jada, J. Douch, Natural Sawdust as Adsorbent for the Eriochrome Black T Dye Removal from Aqueous Solution, *Water Air Soil Pollut.* 230 (2019). <https://doi.org/10.1007/s11270-019-4234-6>.
- Alabarse FG, Conceição RV, Balzaretto NM, Schenato F, Xavier AM (2011) In-situ FTIR analyses of bentonite under high-pressure. *Appl Clay Sci* 51:202–208. <https://doi.org/10.1016/J.CLAY.2010.11.017>
- Alakhras F, Alhajri E, Haounati R, Ouachtak H, Addi AA, Saleh TA, A, (2020) Comparative study of photocatalytic degradation of Rhodamine B using natural-based zeolite composites. *Surf Int* 20:100611. <https://doi.org/10.1016/j.surfint.2020.100611>
- Ayawei N, Ebelegi AN, Wankasi D (2017) Modelling and interpretation of adsorption isotherms. *J Chem* 2017:11. <https://doi.org/10.1155/2017/3039817>
- Azeez L, Lateef A, Adebisi SA, Oyediji AO (2018) Novel biosynthesized silver nanoparticles from cobweb as adsorbent for Rhodamine B: equilibrium isotherm, kinetic and thermodynamic studies. *Appl Water Sci* 8:1–12. <https://doi.org/10.1007/S13201-018-0676-Z/TABLES/4>
- Azeez L, Lateef A, Adejumo AL, Adeleke JT, Adetoro RO, Mustapha Z (2020) Adsorption behaviour of Rhodamine B on hen feather and corn starch functionalized with green synthesized silver nanoparticles (AgNPs) mediated with cocoa pods extracts, chemistry. *Africa* 3:237–250. <https://doi.org/10.1007/S42250-019-00113-7/TABLES/4>
- Azeez L, Adebisi SA, Adejumo AL, Busari HK, Aremu HK, Olabode OA, Awolola O (2022a) Adsorptive properties of rod-shaped silver nanoparticles-functionalized biogenic hydroxyapatite for remediating methylene blue and Congo red. *Inorg Chem Commun* 142:109655. <https://doi.org/10.1016/J.INOCHE.2022.109655>
- Azeez L, Adetoro RO, Busari HK, Aremu HK, Adeleke JT, Adewinbi S, Olabode OA, Ayandayo I (2022b) AgNPs-TiO₂NPs doped calcined hydroxyapatite for effective removal of ibuprofen and acetaminophen. *Int J Environ Analyt Chem*. <https://doi.org/10.1080/03067319.2022.2106434>
- Baskaralingam P, Pulikesi M, Elango D, Ramamurthi V, Sivanesan S (2006) Adsorption of acid dye onto organobentonite. *J Hazard Mater* 128:138–144. <https://doi.org/10.1016/j.jhazmat.2005.07.049>
- Belghiti M, Tanji K, El Mersly L, Lamsayety I, Ouzaouit K, Faqir H, Benzakour I, Rafqah S, Outzourhit A (2022) Fast and non-selective photodegradation of basic yellow 28, malachite green, tetracycline, and sulfamethazine using a nanosized ZnO synthesized from zinc ore. *React Kinet Mech Catal* 135:2265–2278. <https://doi.org/10.1007/S11144-022-02232-8>
- Bello OS, Adegoke KA, Sarumi OO, Lameed OS (2019) Functionalized locust bean pod (*Parkia biglobosa*) activated carbon for Rhodamine B dye removal. *Heliyon* 5:e02323. <https://doi.org/10.1016/j.heliyon.2019.e02323>
- Bello OS, Alabi EO, Adegoke KA, Adegboyega SA, Inyinbor AA, Dada AO (2020) Rhodamine B dye sequestration using *Gmelina aborea* leaf powder. *Heliyon* 6:e02872. <https://doi.org/10.1016/j.heliyon.2019.e02872>
- Bourzi H, Oukhrif R, El Ibrahim B, Oualid HA (2020) Furfural analogs as sustainable corrosion inhibitors—predictive efficiency using DFT and Monte Carlo simulations on the Cu (111), Fe (110), Al (111) and Sn (111) surfaces in acid media. *Sustainability* 12(8):3304
- Bulut Y, Aydin H (2006) A kinetics and thermodynamics study of methylene blue adsorption on wheat shells. *Desalination* 194:259–267
- Chen LF, Wang HH, Lin KY, Kuo JY, Wang MK, Liu CC (2018) Removal of methylene blue from aqueous solution using sediment obtained from a canal in an industrial park. *Water Sci Technol* 78:556–570

- Cheng Z, Feng K, Su Y, Ye J, Chen D, Zhang S, Zhang X, Dionysiou DD (2020) Novel biosorbents synthesized from fungal and bacterial biomass and their applications in the adsorption of volatile organic compounds. *Bioresour Technol* 300:122705. <https://doi.org/10.1016/j.biortech.2019.122705>
- Combes RD, Haveland-Smith RB (1982) A review of the genotoxicity of food, drug and cosmetic colours and other azo, triphenylmethane and xanthene dyes. *Mutat Res* 98:101–243. [https://doi.org/10.1016/0165-1110\(82\)90015-X](https://doi.org/10.1016/0165-1110(82)90015-X)
- Dali Youcef L, Belaroui LS, López-Galindo A (2019) Adsorption of a cationic methylene blue dye on an Algerian palygorskite. *Appl Clay Sci* 179:105145. <https://doi.org/10.1016/j.clay.2019.105145>
- Ddani M, Meunier A, Zahraoui M, Beaufort D, El Wartiti M, Fontaine C, Boukili B, El Mahi B (2005) Clay mineralogy and chemical composition of bentonites from the Gourougou volcanic massif (northeast Morocco). *Clays Clay Miner* 53:250–267. <https://doi.org/10.1346/CCMN.2005.0530305>
- de Souza TNV, de Carvalho SML, Vieira MGA, da Silva MGC, do Brasil DSB (2018) Adsorption of basic dyes onto activated carbon: experimental and theoretical investigation of chemical reactivity of basic dyes using DFT-based descriptors. *Appl Surf Sci* 448:662–670. <https://doi.org/10.1016/j.apsusc.2018.04.087>
- Dhahir SA, Khulood AA-S, Iqbal SA-J (2013) Adsorption study of rhodamine B dye on Iraqi bentonite and modified bentonite by nanocomposites TiO₂, ZnO, Al₂O₃ and sodium dodecyl sulfate. *Am J Sci Environ Sci* 9:269–279
- Dra A, Tanji K, Arrahli A, Iboustaten EM, El Gaidoumi A, Kherchafi A, Chaouni Benabdallah A, Kherbeche A (2020a) Erratum: valorization of Oued Sebou natural sediments (Fez-Morocco Area) as adsorbent of methylene blue dye: kinetic and thermodynamic study. *Sci World J*. <https://doi.org/10.1155/2020/4815767>
- Dra A, Tanji K, Arrahli A, Iboustaten EM, El Gaidoumi A, Kherchafi A, Benabdallah AC, Kherbeche A (2020b) Valorization of oued sebou natural sediments (fez-Morocco area) as adsorbent of methylene blue dye: kinetic and thermodynamic study. *Sci World J* 2020:4815767. <https://doi.org/10.1155/2020/2187129>
- El Bakkali S, Gourgaud A, Bourdier JL, Bellon H, Gundogdu N (1998) Post-collision neogene volcanism of the Eastern Rif (Morocco): magmatic evolution through time. *Lithos* 45:523–543. [https://doi.org/10.1016/S0024-4937\(98\)00048-6](https://doi.org/10.1016/S0024-4937(98)00048-6)
- El Gaidoumi A, Loqman A, Zouheir M, Tanji K, Mertah O, Dra A, El Bali B, Kherbeche A (2021) Sol-gel fluorinated TiO₂-clay nanocomposite: study of fluor-titanium interaction on the photo-degradation of phenol. *Res Chem Intermed* 47:5203–5228. <https://doi.org/10.1007/S11164-021-04573-w>
- El Haouti R, Ouachtak H, El Guerdaoui A, Amedlous A, Amaterz E, Haounati R, Addi AA, Akbal F, El Alem N, Taha ML (2019) Cationic dyes adsorption by Na-Montmorillonite Nano Clay: experimental study combined with a theoretical investigation using DFT-based descriptors and molecular dynamics simulations. *J Mol Liq* 290:111139. <https://doi.org/10.1016/j.molliq.2019.111139>
- El Kassimi A, Achour Y, El Himri M, Laamari R, El Haddad M (2021) Removal of two cationic dyes from aqueous solutions by adsorption onto local clay: experimental and theoretical study using DFT method. *Int J Environ Anal Chem* 103(6):1–22. <https://doi.org/10.1080/03067319.2021.1873306>
- El Miz M, Akichoh H, Berraouan D, Salhi S, Tahani A (2017) Chemical and physical characterization of Moroccan bentonite taken from Nador (North of Morocco). *Am J Chem* 7:105–112
- El Mrabet I, Bellouk H, Bencheqroun Z, Nawdali M, Zaitan H (2021a) Treatment of stabilized landfill leachate using coupled Fenton-like and adsorption process onto Moroccan bentonite clay. *Desalin Water Treat* 240:43–54. <https://doi.org/10.5004/dwt.2021.27754>
- El Mrabet I, Benzina M, Zaitan H (2021b) Treatment of landfill leachate from Fez City by combined Fenton and adsorption processes using Moroccan bentonite clay. *Desalin Water Treat* 225:402–412. <https://doi.org/10.5004/dwt.2021.27142>
- El Mragai A, Daou I, Chfaira R, Zegaoui O (2017) Interfacial electrochemical properties of a Moroccan bentonite in aqueous suspension. *J Mater Environ Sci* 8:3138–3150
- Fahoul Y, Zouheir M, Tanji K, Kherbeche A (2022) Synthesis of a novel ZnAl₂O₄/CuS nanocomposite and its characterization for photocatalytic degradation of acid red 1 under UV illumination. *J Alloys Compd* 889:161708. <https://doi.org/10.1016/j.jallcom.2021.161708>
- Foo KY, Hameed BH (2010) Insights into the modeling of adsorption isotherm systems. *Chem Eng J* 156:2–10. <https://doi.org/10.1016/j.cej.2009.09.013>
- Fullea J, Fernández M, Afonso JC, Vergés J, Zeyen H (2010) The structure and evolution of the lithosphere-asthenosphere boundary beneath the Atlantic-Mediterranean transition region. *Lithos* 120:74–95. <https://doi.org/10.1016/j.lithos.2010.03.003>
- Gupta VK, Ali I, Saini VK (2004) Removal of Rhodamine B, fast green, and methylene blue from wastewater using red mud, an aluminum industry waste. *Ind Eng Chem Res* 43(7):1740–1747
- Hadri M, El Mrabet I, Chaouki Z, Draoui K, Hamdaoui M, Douhri H, Zaitan H (2022) Valorization of natural diatomite mineral: application to removal of anionic dye from aqueous solution in a batch and fixed-bed reactor. *J Cent South Univ* 29:2084–2098. <https://doi.org/10.1007/S11771-022-5065-Y>
- Haounati R, Ouachtak H, El Haouti R, Akhouairi S, Largo F, Akbal F, Benhachemi A, Jada A, Addi AA (2021a) Elaboration and properties of a new SDS/CTAB@Montmorillonite organoclay composite as a superb adsorbent for the removal of malachite green from aqueous solutions. *Sep Purif Technol* 255:117335. <https://doi.org/10.1016/j.seppur.2020.117335>
- Haounati R, El Guerdaoui A, Ouachtak H, El Haouti R, Bouddouch A, Hafid N, Bakiz B, Santos DMF, Labd Taha M, Jada A, Ait Addi A (2021b) Design of direct Z-scheme superb magnetic nanocomposite photocatalyst Fe₃O₄/Ag₃PO₄@Sep for hazardous dye degradation. *Sep Purif Technol* 277:119399. <https://doi.org/10.1016/j.seppur.2021.119399>
- Haounati R, Alakhras F, Ouachtak H, Saleh TA, Al-Mazaideh G, Alhajri E, Jada A, Hafid N, Addi AA (2022) Synthesized of Zeolite@Ag₂O nanocomposite as superb stability photocatalysis toward hazardous Rhodamine B dye from water. *Arab J Sci Eng*. <https://doi.org/10.1007/s13369-022-06899-y>
- Heibati B, Rodriguez-Couto S, Amrane A, Rafatullah M, Hawari A, Al-Ghouti MA (2014) Uptake of reactive Black 5 by pumice and walnut activated carbon: chemistry and adsorption mechanisms. *J Ind Eng Chem* 20:2939–2947. <https://doi.org/10.1016/j.jiec.2013.10.063>
- Hou M, Ma C, Zhang W, Tang X, Fan Y, Wan H (2011) Removal of rhodamine B using iron-pillared bentonite. *J Hazard Mater* 186:1118–1123
- Hu QH, Qiao SZ, Haghseresht F, Wilson MA, Lu GQ (2006) Adsorption study for removal of basic red dye using bentonite. *Ind Eng Chem Res* 45(2):733–738
- Huang Z, Li Y, Chen W, Shi J, Zhang N, Wang X, Li Z, Gao L, Zhang Y (2017) Modified bentonite adsorption of organic pollutants of dye wastewater. *Mater Chem Phys* 202:266–276. <https://doi.org/10.1016/j.matchemphys.2017.09.028>
- Inyinbor AA, Adekola FA, Olatunji GA (2016) Kinetics, isotherms and thermodynamic modeling of liquid phase adsorption of Rhodamine B dye onto *Raphia hookeri* fruit epicarp. *Water Resour Ind* 15:14–27. <https://doi.org/10.1016/j.wri.2016.06.001>
- Jiang N, Erdős M, Moulton OA, Shang R, Vlught TJH, Heijman SGJ, Rietveld LC (2020) The adsorption mechanisms of organic micropollutants on high-silica zeolites causing S-shaped adsorption isotherms: an experimental and Monte Carlo simulation study. *Chem Eng J* 389:1239698. <https://doi.org/10.1016/j.cej.2019.123968>

- Kausar A, Naeem K, Tariq M, Nazli ZIH, Bhatti HN, Jubeen F, Nazir A, Iqbal M (2019) Preparation and characterization of chitosan/clay composite for direct rose FRN dye removal from aqueous media: comparison of linear and non-linear regression methods. *J Market Res* 8:1161–1174. <https://doi.org/10.1016/j.jmrt.2018.07.020>
- Khan TA, Dahiya S, Ali I (2012) Use of kaolinite as adsorbent: Equilibrium, dynamics and thermodynamic studies on the adsorption of Rhodamine B from aqueous solution. *Appl Clay Sci* 69:58–66
- Khudhair A, Rudaini AL (2017) Adsorption removal of Rhodamine-B Dye from aqueous solution using Rhamnus stone as low cost adsorbent. *J Al-Nahrain Univ Sci* 20:32–41
- Kirkpatrick S, Gelatt CD, Vecchi MP (1979) Optimization by simulated annealing. *Science* 220(1983):671–680. <https://doi.org/10.1126/science.220.4598.671>
- Laabd M, Brahmī Y, El Ibrahimī B, Hsini A, Toufik E, Abdellaoui Y, Abou Oualid H, El Ouardi M, Albourine A (2021) A novel mesoporous Hydroxyapatite@Montmorillonite hybrid composite for high-performance removal of emerging Ciprofloxacin antibiotic from water: integrated experimental and Monte Carlo computational assessment. *J Mol Liq* 338:116705. <https://doi.org/10.1016/j.molliq.2021.116705>
- Lamrani O, Aabi A, Boushaba A, Seghir MT, Adiri Z, Samaoui S (2021) Bentonite clay minerals mapping using ASTER and field mineralogical data: a case study from the eastern Rif Belt Morocco. *Remote Sens Appl* 24:100640. <https://doi.org/10.1016/j.rsase.2021.100640>
- Leodopoulos C, Doulia D, Gimouhopoulos K, Triantis TM (2012) Single and simultaneous adsorption of methyl orange and humic acid onto bentonite. *Appl Clay Sci* 70:84–90
- Lian L, Guo L, Guo C (2009) Adsorption of Congo red from aqueous solutions onto Ca-bentonite. *Hazard Mater J* 161:126–131. <https://doi.org/10.1016/j.jhazmat.2008.03.063>
- Mbognou MHT, Lambert SD, Caucheteux J, Farcy A, Alié C, Fagel N, Woumfo ED, Mahy JG (2022) Hybrid clay-based materials for organic dyes and pesticides elimination in water. *J Solgel Sci Technol* 105:461–470. <https://doi.org/10.1007/s10971-022-06005-6>
- Mohamed M, Ouki S (2011) Removal mechanisms of toluene from aqueous solutions by chitin and chitosan. *J Water Air Soil Pollut* 50:9557–9563
- Namasivayam C, Kavitha D (2002) Removal of Congo Red from water by adsorption onto activated carbon prepared from coir pith, an agricultural solid waste. *J Dyes Pigment* 54:47–58
- Ouachtak H, Akhouairi S, Haounati R, Addi AA, Jada A, Taha ML, Douch J (2020) 3,4-Dihydroxybenzoic acid removal from water by goethite modified natural sand column fixed-bed: experimental study and mathematical modeling. *Desalin Water Treat* 194:439–449
- Ouachtak H, El Haouti R, El Guerdaoui A, Haounati R, Amaterz E, Addi AA, Akbal F, Taha ML (2020) Experimental and molecular dynamics simulation study on the adsorption of Rhodamine B dye on magnetic montmorillonite composite $\gamma\text{-Fe}_2\text{O}_3\text{@Mt}$. *J Mol Liq* 309:113142. <https://doi.org/10.1016/j.molliq.2020.113142>
- Oyekanmi AA, Ahmad A, Hossain K, Rafatullah M (2019) Statistical optimization for adsorption of Rhodamine B dye from aqueous solutions. *J Mol Liq* 281:48–58. <https://doi.org/10.1016/j.molliq.2019.02.057>
- Qabaqous O, Tijani N, Bennani MN, El Krouk A (2014) Elaboration et caractérisation des supports plans à base d'argile (Rhassoul) pour membranes minérales (Préparation and characterization of supports plans from the (Rhassoul) clay for mineral membranes). *J Mater Environ Sci* 5:2244–2249
- Qlihaa A, Dhimni S, Melrhaka F, Hajjaji N, Srhiri A (2016) Caractérisation physico-chimique d'une argile Marocaine [Physico-chemical characterization of a Moroccan clay]. *J Mater Environ Sci* 7:1741–1750
- Rabti A, Hannachi A, Maghraoui-Meherzi H, Raouafi N (2019) Ferrocene-functionalized carbon nanotubes: an adsorbent for Rhodamine B, chemistry. *Africa* 2:113–122. <https://doi.org/10.1007/S42250-018-00031-0/FIGURES/7>
- Reddy CR, Bhat YS, Nagendrappa G, Prakash BSJ (2009) Brønsted and Lewis acidity of modified montmorillonite clay catalysts determined by FT-IR spectroscopy. *Catal Today* 141:157–160
- Senthil Kumar P, Ramalingam S, Senthamarai C, Niranjana M, Vijayalakshmi P, Sivanesan S (2010) Adsorption of dye from aqueous solution by cashew nut shell: Studies on equilibrium isotherm, kinetics and thermodynamics of interactions. *J Des* 261:52–60
- Singh KP, Mohan D, Sinha S, Tondon GS, Gosh D (2003) Color removal from wastewater using low-cost activated carbon derived from agricultural waste material. *Ind Eng Chem Res* 42(9):1965–1976
- Singh S, Parveen N, Gupta H (2018) Adsorptive decontamination of rhodamine-B from water using banana peel powder: a biosorbent. *Environ Technol Innov* 12:189–195. <https://doi.org/10.1016/J.ETI.2018.09.001>
- Tanji K, El Mrabet I, Fahoul Y, Jellal I, Benjelloun M, Belghiti M, El Hajam M, Naciri Y, El Gaidoumi A, El Bali B, Zaitan H, Kherbeche A (2023a) Epigrammatic progress on the photocatalytic properties of ZnO and TiO₂ based hydroxyapatite@photocatalyst toward organic molecules photodegradation: a review. *J Water Proc Eng* 53:103682. <https://doi.org/10.1016/J.JWPE.2023.103682>
- Tanji K, Fahoul Y, El Mrabet I, Zaitan H, Kherbeche A (2023b) Combined natural mineral@ZnCoO system for photocatalytic degradation of malachite green under visible radiation. *Chem Afr*. <https://doi.org/10.1007/S42250-023-00598-3>
- Tanji K, El Mrabet I, Fahoul Y, Soussi A, Belghiti M, Jellal I, Naciri Y, El Gaidoumi A, Kherbeche A (2023c) Experimental and theoretical investigation of enhancing the photocatalytic activity of Mg doped ZnO for nitrophenol degradation. *React Kinet Mech Cataly*. <https://doi.org/10.1007/S11144-023-02385-0>
- Taylor P, Feddal I, Ramdani A, Taleb S, Gaigneaux EM, Batis N, Ghaffour N (2014) Adsorption capacity of methylene blue, an organic pollutant, by montmorillonite clay. *Desalin Water Treat* 52(13–15):37–41
- Thiam A, Tanji K, Assila O, Zouheir M, Haounati R, Arrahli A, Abeid A, Lairini S, Bouslamti R, Zerouq F, Kherbeche A (2020) Valorization of date pits as an effective biosorbent for remazol brilliant blue adsorption from aqueous solution. *J Chem*. <https://doi.org/10.1155/2020/4173152>
- Toor M, Jin B, Dai S, Vimonses V (2015) Activating natural bentonite as a cost-effective adsorbent for removal of Congo-red in wastewater. *J Ind Eng Chem* 21:653–661. <https://doi.org/10.1016/j.jiec.2014.03.033>
- Vakili M, Rafatullah M, Salamatinia B, Abdullah AZ, Ibrahim MH, Tan KB, Gholami Z, Amouzgar P (2014) Application of chitosan and its derivatives as adsorbents for dye removal from water and wastewater: a review. *Carbohydr Polym* 113:115–130. <https://doi.org/10.1016/j.carbpol.2014.07.007>
- Verma AK, Dash RR, Bhunia P (2012) A review on chemical coagulation/flocculation technologies for removal of colour from textile wastewaters. *J Environ Manage* 93:154–168. <https://doi.org/10.1016/j.jenvman.2011.09.012>

Publisher's Note Springer Nature remains neutral with regard to jurisdictional claims in published maps and institutional affiliations.

Springer Nature or its licensor (e.g. a society or other partner) holds exclusive rights to this article under a publishing agreement with the author(s) or other rightsholder(s); author self-archiving of the accepted manuscript version of this article is solely governed by the terms of such publishing agreement and applicable law.